eprints@whiterose.ac.uk
https://eprints.whiterose.ac.uk/

Supplementary Information

1   Molecular Weight and Polydispersity Characterisation of Flow-Synthesised P3HT

Size-Exclusion Chromatography (SEC) was performed using an Agilent 1200 Series GPC-SEC Analysis System fitted with two PLgel mixed-B columns in series running a chlorobenzene eluent and calibrated to polystyrene standards. All samples were filtered with a 0.2 μm PTFE filter to remove particulate matter. Polymer eluted between 14 and 18 minutes. The chromatogram acquired for P3HT (Mw = 60 kg/mol) is shown in Figure 1.
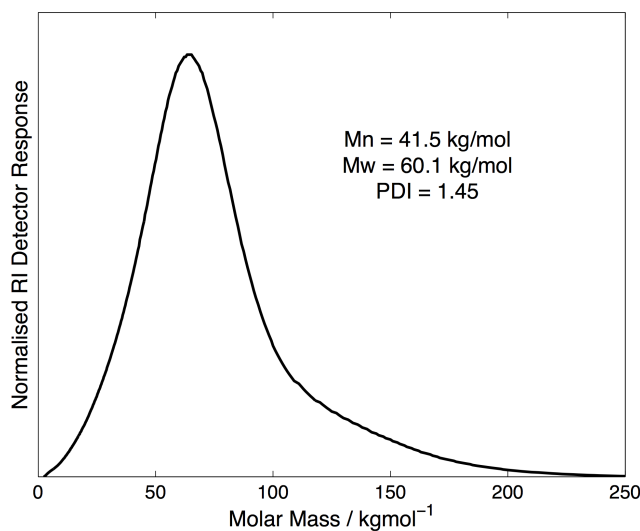
Figure 1 Size-Exclusion Chromatogram for P3HT in chlorobenzene.

2   Regioregularity Characterisation of Flow-Synthesised P3HT

Nuclear Magnetic Resonance (NMR) was performed on a Bruker AV-400 NMR machine (400 MHz). 1H NMR was recorded in the range 0-10 ppm against a TMS reference. Regioregularity was determined from the ratio of the methylene proton integrals at 2.60 ppm (ir) and 2.84 ppm (r) using the formula: $\frac{r}{ir+r} \times 100\%$. NMR spectra are shown in Figure 2.
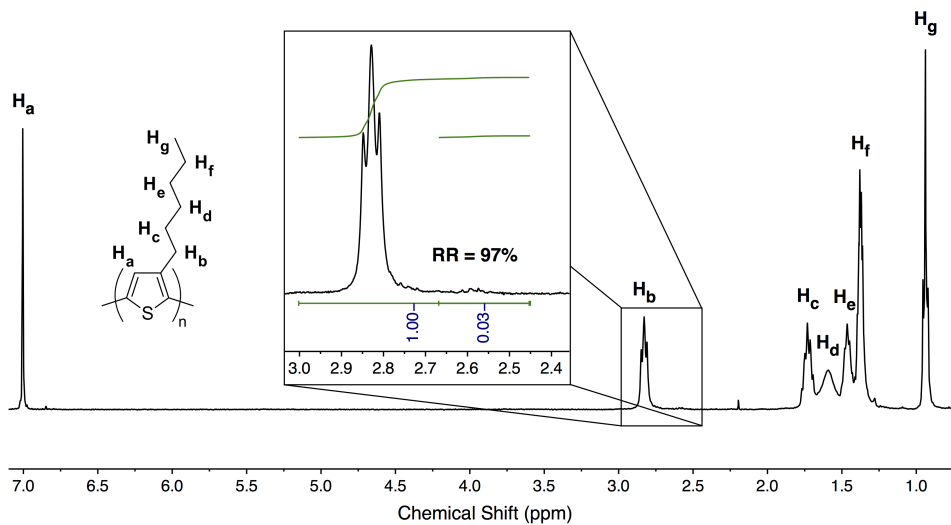
Figure 2 NMR spectra for flow-synthesised P3HT with Mw = 60 kg/mol. The chemical shifts are labeled for each proton, and the inset details the integration region used to calculate the regioregularity.

2

3   Neutron Scattering Length Densities (SLD's)

species	atomic formula	density (g/cm^3)	SLD (cm^{-2})
P3HT, crystalline	$C_{10}H_{14}S$	1.12	6.9 x 10^9
P3HT, amorphous	$C_{10}H_{14}S$	1.09	6.7 x 10^9
PCBM	$C_{72}H_{14}O_2$	1.5	4.3 x 10^{10}

Table 1 Physical characteristics of P3HT and PCBM. Atomic scattering lengths were taken from the compendium produced by V.F. Sears [1].

4   Details of SANS Fitting

The scattering length density contrast between P3HT crystals and the matrix is defined for a constant value of the SLD of crystalline P3HT, $\rho_{P3HT,c} = 6.9 \times 10^9$ cm^{-2}.

$$\Delta\rho = |\rho_{P3HT,c} - \rho_{matrix}| \tag{1}$$

The scattering length density of the matrix is presumed to comprise contributions proportional to the volume fractions of amorphous P3HT and PCBM.

$$\rho_{matrix} = \frac{\rho_{P3HT,am}\phi_{P3HT,am} + \rho_{PCBM}\phi_{PCBM}}{\phi_{P3HT,am} + \phi_{PCBM}} \tag{2}$$

The denominator in Eqn 2 normalises the contribution of each species in the matrix to the total volume fraction of the sample composed of the mixed matrix phase. The volume fraction of each component is constrained by:

$$1 = \phi_{P3HT,c} + \phi_{P3HT,am} + \phi_{PCBM} \tag{3}$$

The mass fraction of P3HT in the sample is fixed by the experimental conditions, for the samples studied by SANS, $x_{P3HT} = 0.75$, where it is useful to decompose the total mass fraction of P3HT into crystalline and amorphous components.

$$\frac{x_{P3HT,c} + x_{P3HT,am}}{x_{P3HT,c} + x_{P3HT,am} + x_{PCBM}} = 0.75 \tag{4}$$

Given a fitted value of $\phi_{P3HT,c}$, the resulting value of $\Delta\rho$ can be calculated from the above equations by noting that the mass fraction of each component is related to the volume fraction by the material densities, ρ^{mat}.

$$x_i = \frac{\phi_i \rho_i^{mat}}{\sum_i \phi_i \rho_i^{mat}} \tag{5}$$

For the experimental constraint used in this study, $x_{P3HT} = 0.75$, the correlation between scattering contrast and crystalline P3HT volume fraction is shown in Fig 3.
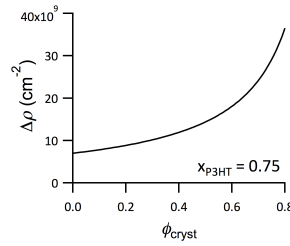
Figure 3 Scattering length density contrast, $\Delta\rho = |\rho_{P3HT,c} - \rho_{matrix}|$, as a function of the volume fraction of crystalline P3HT, $\phi_{P3HT,c}$, for blends containing a total mass fraction of P3HT, $x_{P3HT} = 0.75$

5   SANS data acquired during thermal annealing
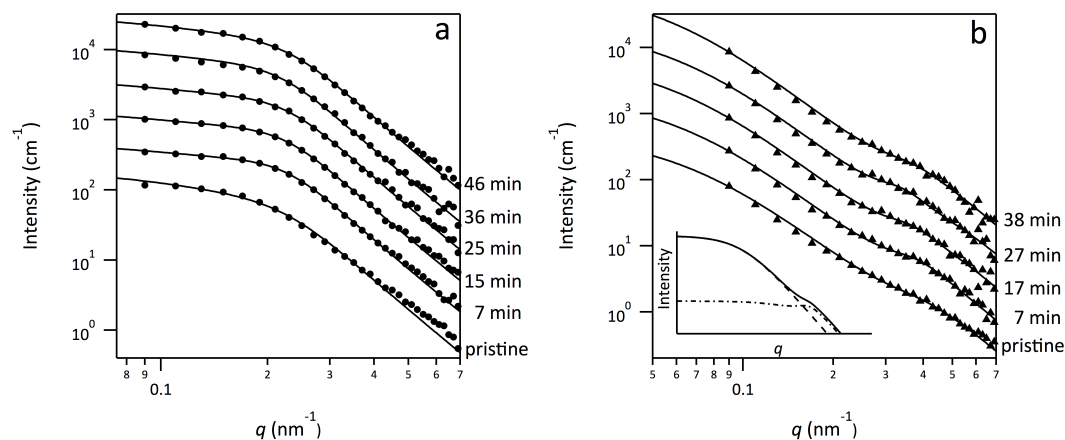
Figure 4 SANS spectra for P3HT:PCBM blends (25 wt% PCBM) acquired during a thermal anneal at 140 °C for a (a) drop cast and (b) rapid precipitation sample. The solid lines in (a) are fits to a polydisperse hard sphere form and structure factor. The solid lines in (b) are fits to a summed structure factor comprising a polydisperse hard sphere partial structure factor to model the P3HT crystals and a DAB partial structure factor to model the PCBM aggregates. The inset shows the total structure factor (—) for RP25 at 38 min decomposed into contributions from the DAB (- - -) and hard spheres (- · -). The two pristine spectra were measured at 25 °C prior to any thermal treatment, all other spectra were measured at 140 °C. The pristine spectra are located at the absolute intensity value, each subsequent spectrum is shifted 3000 cm^{-1} from the spectrum immediately below it.

Table 2 Polydisperse hard sphere fitting parameters and Porod power laws for the SANS spectra of a P3HT:PCBM blend (25 wt%) prepared by drop casting. Fits were performed during an anneal at 140 °C.

Drop Cast	Pristine	Annealing at 140 °C					melt-quenched
Elapsed time (min)	0	7	15	25	36	46	—
P3HT crystal radius (nm)	7.8	10.2	10.2	9.6	9.5	8.4	9.2
Volume fraction of P3HT crystals	0.45	0.51	0.51	0.49	0.47	0.46	0.60
Polydispersity of P3HT crystals	0.62	0.48	0.49	0.50	0.52	0.56	0.58
$\Delta\rho$ (1 x 10^{-10} cm^{-2})	1.31	1.47	1.45	1.42	1.36	1.32	1.27
x_{PCBM}^{am}	0.44	0.49	0.49	0.47	0.45	0.45	0.10
Porod power law for P3HT crystals	-3.75	-4.02	-4.10	-4.11	-4.21	-3.93	-4.47
($\pm$)	0.11	0.10	0.09	0.13	0.10	0.10	0.06

5

Table 3 Porod law powers, DAB parameters, and hard sphere fitting parameters of SANS spectra measured for a rapid precipitation P3HT:PCBM blend (25 wt% PCBM) during a thermal anneal at 140 °C and after a melt-quench. The measurement at 0 min was performed at 25 °C, that of the melt-quench at 35 °C, and all others at 140 °C.

Rapid Precipitation	Pristine	Annealing at 140 °C				melt-quenched
Elapsed time (min)	0	7	17	28	38	—
Temperature (°C)	25	140	140	140	140	35
Porod power law for PCBM aggregates	-3.12	-3.17	-3.21	-3.18	-3.33	—
($\pm$)	0.02	0.02	0.01	0.01	0.01	—
Porod power law for P3HT crystals	-2.75	-3.28	-3.33	-3.02	-3.43	-4.64
($\pm$)	0.04	0.23	0.09	0.15	0.67	0.07
DAB scale (cm^{-1}nm^{-3})	0.185	0.203	0.206	0.206	0.212	0.440
DAB ξ (nm)	14.0	14.8	15.6	15.4	16.6	24.4
P3HT crystal radius (nm)	7.5	8.2	9.0	10.3	8.5	9.1
Volume fraction of P3HT crystals	0.69	0.66	0.70	0.74	0.69	0.50
Polydispersity of P3HT crystals	0.43	0.34	0.32	0.29	0.37	0.40
$\Delta\rho$ (1 x 10^{-10} cm^{-2})	0.56	0.55	0.56	0.60	0.54	1.32
x_{PCBM}^{am}	0.05	0.05	0.04	0.03	0.05	0.10

6   SANS fits to coexisting PCBM aggregates and P3HT crystals
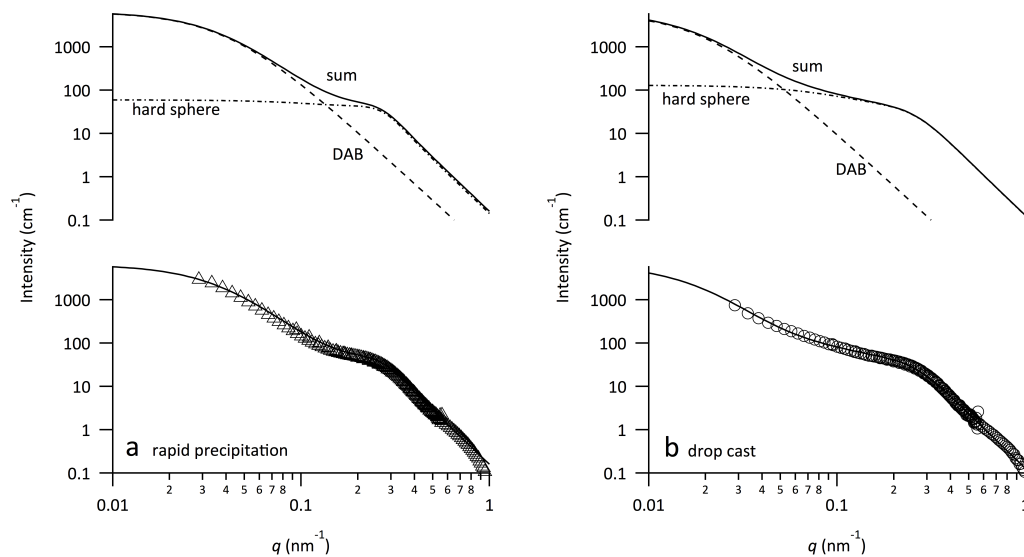
Figure 5 SANS spectra for P3HT:PCBM blends (25 wt% PCBM) prepared by (a) rapid precipitation (△) and (b) drop casting (○). A possible decomposition of the total structure factor (—) into the partial structure factors for a Debye-Anderson-Brumberger two-phase system (- - -) and polydisperse hard spheres (- · -) is shown on the top axes; the fitted total structure factor and data are shown on the bottom axes.

7

7 XRD fitting

XRD data were fitted to obtain the Scherrer length, L_c, in the [h00] crystal direction of P3HT, as well as the peak areas, known to correlate with degree of crystallinity. The background subtraction, shown in Figure 6a, comprised an amorphous contribution and a low q exponential decay. The shape of the amorphous contribution was measured from an amorphous sample, fitted with a high order polynomial, and scaled to coincide with the measured baseline for each sample. The exponential contribution was fitted to the low q upturn. The resulting profile, with a flattened baseline, is shown in Figure 6b. The peaks were fitted with the pseudo Voigt model (shown in Figure 6c):

$$I(q) = \eta \frac{1}{1 + \left(\frac{q - q_{peak}}{\Delta_q}\right)^2} + (1 - \eta) exp\left[-\frac{q - q_{peak}}{\Delta_q}\right]^2 \tag{6}$$
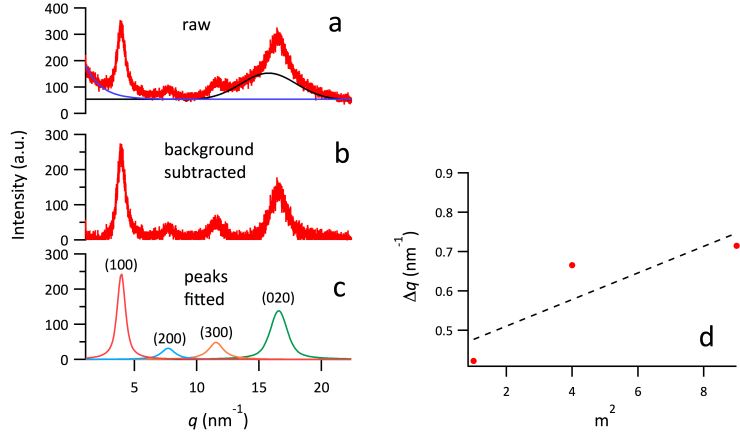
Figure 6 XRD data correction and fitting for a P3HT sample prepared by rapid precipitation. (a) The raw spectrum (—) is shown with the exponential (—) and amorphous (—) background corrections. (b) The background-subtracted spectrum. (c) Pseudo Voigt fits to the corrected spectrum with peak orders labelled. (d) Peak widths (●) versus the peak order squared to determine the Scherrer length by linear extrapolation (- - -).

The fitted values for the width of the peak, Δ_q are plotted against the square of the peak order, m^2, for the [h00] direction and extrapolated to $m^2 = 0$, as shown in Figure 6d. Following the analysis of Rivnay et al.[2], the extrapolation of Δ_q to zero is used to calculate $L_c = \frac{2\pi K}{\Delta_q}$. The points are not exceptionally collinear due to the large uncertainties in the fits of the (200) and (300) peaks ($R^2 = 0.76$, compared to $R^2 = 0.99$ for the P(NDI2OD-T2) data measured and listed in Table 1 of the Rivnay et al. paper[2].) We have chosen to calculate the Scherrer length, L_c, based solely upon the (100) peak because it exhibits the largest signal to noise, and not all samples exhibit all three reflections needed for an extrapolation. Using the extrapolation we calculate $L_c = 12.8 \pm 4.2$ nm, and using just the first order peak with $L_c = \frac{2\pi K}{\Delta_q cos\theta_{100}}$ and $\theta_{100} = 2 sin^{-1}(q_{peak}\lambda/4\pi)$, $\lambda = 0.154$ nm, K =0.9, we calculate $L_c = 13.4 \pm 0.3$ nm.

Table 4 XRD parameters fitted and calculated for the spectrum of P3HT prepared by rapid precipitation

Peak	RP-P3HT			RP25		
	q_{peak} (nm^{-1})	Δ_q (nm^{-1})	L_c (nm)	q_{peak} (nm^{-1})	Δ_q (nm^{-1})	L_c (nm)
(100)	3.94	0.42 ± 0.01	13.4 ± 0.30	3.99	0.40 ± 0.01	14.1 ± 0.18
(200)	7.70	0.67 ± 0.09	8.7 ± 1.02	7.71	0.54 ± 0.04	10.7 ± 0.77
(300)	11.5	0.71 ± 0.06	8.2 ± 0.68	11.7	0.73 ± 0.06	8.0 ± 0.58
(020)	16.2	0.90 ± 0.02	6.8 ± 0.18	16.7	0.44 ± 0.05	14.0 ± 1.49

8   XRD for pristine rapid precipitation P3HT and blended P3HT:PCBM (25 wt% PCBM)
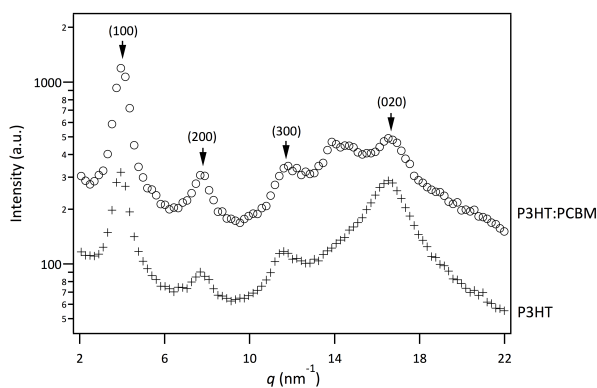
Figure 7 XRD spectra for pristine rapid precipitation samples comprising pure P3HT (+) and a blend of P3HT:PCBM with 25 wt% PCBM (○). The first 3 Bragg reflections of the P3HT (100) peak are indicated along with the (020) peak. The shoulder at 14 nm^{-1} is due to PCBM, but cannot be distinctly identified with either the crystalline or amorphous form as it is present in both cases [3].

9   DSC profiles and transition temperatures
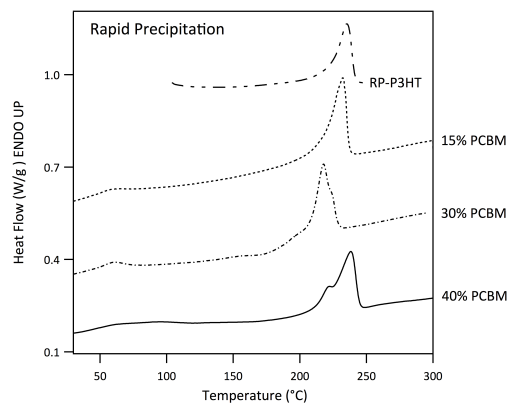
Figure 8 DSC first heating profiles for P3HT:PCBM blends prepared by rapid precipitation for concentrations of 0-40 wt% PCBM.

Table 5 DSC measurements of T_m and T_c reported in °C for the first (pristine) and second thermal cycles, denoted with subscripts 1 and 2, respectively. Uncertainties for all measurements are $\pm$ 1 °C.

Sample	$T_{m,1}$	$T_{c,1}$	$T_{m,2}$	$T_{c,2}$
RP-P3HT	241	210	241	—
RP15	238	196	231	193
DC15	237	194	232	192
RP30	230	182	226	179
DC30	228	178	226	176
RP40	241	190	234	191

10 Muon Spectroscopy

The interface between a PCBM aggregate and the mixed phase exhibits subtle differences if the PCBM is amorphous or crystalline. Muon spin resonance (μSR) is a sensitive way to distinguish between similar atomic environments with small chemical or structural differences. A pulse of spin-polarised muons is implanted into the sample, and in the case of semiconductors, forms an unstable intermediate known as muonium. In the presence of a magnetic field, the local magnetic environment depolarises the Larmor precession of muonium spins. The resulting phase asymmetry of the decay product is measured as a function of the applied magnetic field.

Figure 9a shows the fractional asymmetry as a function of the magnetic field for RP40 before and after melting the sample at 245 °C. The small differences between the spectra are quite significant, and must be interpreted with respect to the known spectra of the pure components. Figure 9b shows the quotient of the pristine and annealed spectra. Regions in the magnetic field associated with the resonance of the PCBM ligand, cage, and P3HT have been previously identified [4] and are indicated. Where the quotient is greater than unity there is an increase in the fraction of chemical species associated with the resonance, and conversely, a quotient less than unity indicates a depletion of the chemical species. There is no apparent change in the chemical environment of P3HT before and after annealing, in agreement with the observation of P3HT crystals in the pristine and annealed samples. However, there is an increase in the fraction of PCBM ligands that react to form muonium, and a simultaneous decrease in the number of PCBM cages that form muonium. In general, muons react at the interface of crystals rather than penetrating within the lattice. The PCBM crystal unit cell is known to exhibit centrally located cages with protruding ligands, so that an excess of PCBM ligands exist at the interface of a PCBM crystal. The increased muonium implantation in PCBM ligands combined with the decrease in implantation in cages suggests that PCBM is more crystalline in the annealed sample.
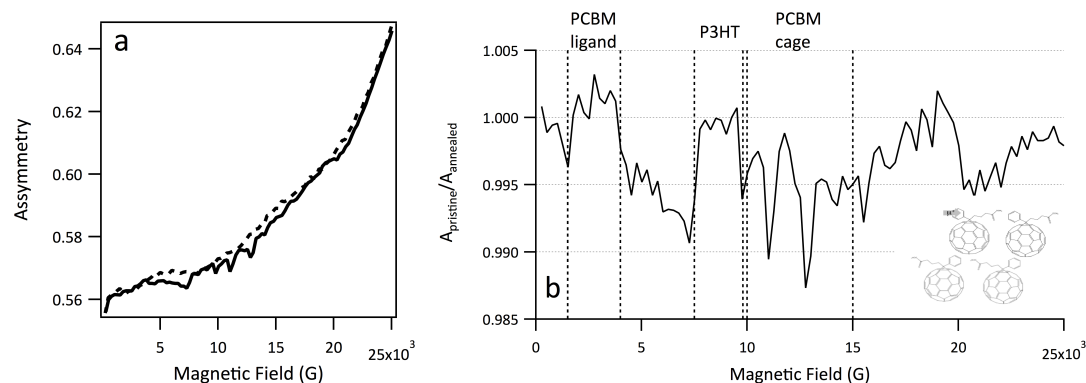
Figure 9 Muon spin resonance measurements for a P3HT:PCBM (40 wt% PCBM) blend (a) before (——) and after (- - -) a melting anneal. Asymmetry of the positron decay is shown as a function of applied magnetic field. (b) Ratio of the pristine and annealed spectra, with resonant windows labeled. Schematic shows potential location for muon implantation at the interface of a PCBM lattice.

11

References

[1] Varley F Sears. Neutron scattering lengths and cross sections. *Neutron News*, 3(3):26–37, 1992.

[2] Jonathan Rivnay, Rodrigo Noriega, R. Joseph Kline, Alberto Salleo, and Michael F. Toney. Quantitative analysis of lattice disorder and crystallite size in organic semiconductor thin films. *Physical Review B*, 84(4):045203, July 2011.

[3] Paul E. Hopkinson, Paul A. Staniec, Andrew J. Pearson, Alan D. F. Dunbar, Tao Wang, Anthony J. Ryan, Richard A. L. Jones, David G. Lidzey, and Athene M. Donald. A Phase Diagram of the P3HT:PCBM Organic Photovoltaic System: Implications for Device Processing and Performance. *Macromolecules*, 44(8):2908–2917, April 2011.

[4] Francis Pratt. *personal communication*, 2014.